EBioMedicine 49 (2019) 305–317

Contents lists available at ScienceDirect

EBioMedicine

journal homepage: www.elsevier.com/locate/ebiom

Research paper

Activation of sonic hedgehog signaling by a Smoothened agonist restores congenital defects in mouse models of endocrine-cerebro-osteodysplasia syndrome

Jeong-Oh Shin[a,†], Jieun Song[f,†], Han Seul Choi[a,c], Jisu Lee[e], Kyeong Lee[e], Hyuk Wan Ko[f,*], Jinwoong Bok[a,b,c,d,*]

[a] Department of Anatomy, Yonsei University College of Medicine, Seoul 03722, Korea
[b] Department of Otorhinolaryngology, Yonsei University College of Medicine, Seoul 03722, Korea
[c] BK21 PLUS project for Medical Science, Yonsei University College of Medicine, Seoul 03722, Korea
[d] Severance Biomedical Science Institute, Yonsei University College of Medicine, Seoul 03722, Korea
[e] College of Pharmacy, Dongguk University, Goyangsi, Gyeonggido, 10326, Korea
[f] Department of Biochemistry, College of Life Science and Biotechnology, Yonsei University, Seoul 03722, Korea

ARTICLE INFO

Article history:
Received 17 June 2019
Revised 30 September 2019
Accepted 9 October 2019
Available online 26 October 2019

Keywords:
Cleft palate
Ciliopathy, Sonic hedgehog
Endocrine-cerebro-osteodysplasia (ECO) syndrome
Smoothened agonist (SAG)

ABSTRACT

Background: Endocrine-cerebro-osteodysplasia (ECO) syndrome is a genetic disorder associated with congenital defects of the endocrine, cerebral, and skeletal systems in humans. ECO syndrome is caused by mutations of the intestinal cell kinase (*ICK*) gene, which encodes a mitogen-activated protein (MAP) kinase-related kinase that plays a critical role in controlling the length of primary cilia. Lack of ICK function disrupts transduction of sonic hedgehog (SHH) signaling, which is important for development and homeostasis in humans and mice. Craniofacial structure abnormalities, such as cleft palate, are one of the most common defects observed in ECO syndrome patients, but the role of ICK in palatal development has not been studied.

Methods: Using *Ick*-mutant mice, we investigated the mechanisms by which ICK function loss causes cleft palate and examined pharmacological rescue of the congenital defects.

Findings: SHH signaling was compromised with abnormally elongated primary cilia in the developing palate of *Ick*-mutant mice. Cell proliferation was significantly decreased, resulting in failure of palatal outgrowth, although palatal adhesion and fusion occurred normally. We thus attempted to rescue the congenital palatal defects of *Ick* mutants by pharmacological activation of SHH signaling. Treatment of *Ick*-mutant mice with an agonist for Smoothened (SAG) rescued several congenital defects, including cleft palate.

Interpretations: The recovery of congenital defects by pharmacological intervention in the mouse models for ECO syndrome highlights prenatal SHH signaling modulation as a potential therapeutic measure to overcome congenital defects of ciliopathies.

Research in Context

Evidence before this study

Endocrine-cerebro-osteodysplasia (ECO) syndrome is caused by mutations in the intestinal cell kinase (*ICK*) gene in humans. Previous studies suggested that ICK protein plays a crucial role in controlling the length of primary cilia, which act as control towers for various signaling pathways essential for animal development and homeostasis. Among many signaling pathways that are dependent on primary cilia, key SHH signaling components are shown to be mislocalized within the elongated or shortened primary cilia and proposed to be a major reason for the congenital defects exhibited in ECO syndrome. Mouse models carrying mutations in the *Ick* gene recapitulate the spectrum of human ECO syndrome developmental anomalies, including cleft palate, hydrocephalus, polydactyly, and skeletal defects; however, it is not entirely clear whether disrupted SHH signaling is the sole reason for

* Correspondence author.
E-mail addresses: kohw@yonsei.ac.kr (H.W. Ko), bokj@yuhs.ac (J. Bok).
† These authors contributed equally to this work.

https://doi.org/10.1016/j.ebiom.2019.10.016

developmental defects caused by ICK deficiency in ECO syndrome patients and mouse models.

Added value of this study

To test whether compromised SHH signaling is the major cause of congenital anomalies in *Ick* mutants, we used cleft palate as a model system because it is one of the most common defects observed in ECO syndrome patients and *Ick*-mutant mice. We first found that SHH signaling is indeed compromised in the developing palatal tissues in *Ick*-mutant mice. The reduced SHH signaling appeared to cause a decrease in cell proliferation, leading to failure of palatal-shelf outgrowth. The two palatal shelves remained separated at either side, resulting in cleft palate. If disrupted SHH signaling due to abnormal cilia is indeed the key cause of the cleft palate, re-activation of the compromised SHH signaling in *Ick* mutants could rescue the cleft palate defect. We tested this hypothesis by activating SHH signaling in developing mouse embryos using a small molecule SHH agonist (SAG). We observed that SAG injection into pregnant mice rescued multiple congenital defects, including cleft palate, in *Ick*-mutant embryos, indicating that SHH signaling is indeed the main effector that is compromised by abnormal cilia and leads to congenital anomalies in *Ick*-mutant mice.

Implications of all the available evidence

These results provide *in vivo* evidence that disrupted SHH signaling is the primary cause of abnormal craniofacial development in ECO syndrome. Furthermore, our demonstration of the rescue of cleft palate by pharmacological intervention suggests that prenatal modulation of developmental signaling using a small chemical compound may provide a therapeutic option for rescuing congenital defects in genetic diseases, such as ciliopathies.

1. Introduction

Endocrine-cerebro-osteodysplasia (ECO) syndrome [MIM:612651] is a recessive genetic disorder associated with multiple congenital defects in the endocrine, cerebral, and skeletal systems in humans [1]. ECO syndrome is caused by mutations in the intestinal cell kinase (*ICK*) gene [1–3]. Mouse models carrying mutations in the *Ick* gene recapitulate the spectrum of developmental anomalies, including cleft palate, hydrocephalus, polydactyly, delayed skeletal development, and abnormal lung development, observed in human ECO patients [3–5]. ICK has been shown to play a critical role in the regulation of primary cilia length. Thus, abnormal ICK function results in abnormally elongated primary cilia and leads to disrupted sonic hedgehog (SHH) signal transduction [3, 4]. SHH target genes, such as *Gli1* and *Ptch1*, are downregulated in the mesenchyme of developing limb buds, growth plates, and perichondrium in *Ick*-mutant embryos [3, 4]. These results suggest that abnormal SHH signaling is a major pathological mechanism underlying the developmental defects caused by ICK deficiency in humans and mice.

Congenital craniofacial abnormalities, such as cleft palate/lip, are one of the most common defects observed in ECO syndrome [1]. Palatal development depends on reciprocal interactions between palatal ectoderm and underlying mesenchyme, and SHH is an important epithelial signal that promotes palatal outgrowth [6]; however, it has not been directly examined whether abnormal ciliary elongation and the resultant reduced SHH signaling are indeed major causes of cleft palate in ECO syndrome.

Currently, it is not feasible to correct developmental defects, such as ECO syndrome or other ciliopathies that are caused by genetic mutations. Several attempts have been made to rescue congenital defects using pharmacological interventions that either activate or inhibit causative signaling pathways affected by the genetic mutations. Aortic aneurysm in Marfan syndrome, a genetic disorder caused by mutations in the fibrillin 1 (*FBN1*) gene, can be rescued by treatment with losartan, an angiotensin II type 1 receptor blocker [7]. In addition, treatment with rapamycin significantly alleviates the polycystic kidney phenotype in zebrafish ciliopathy models, mouse models for polycystic kidney disease (PKD), and human autosomal-dominant PKD (ADPKD) patients [8, 9]. Furthermore, treatment with dantrolene, an inhibitor of the endoplasmic reticulum (ER)-localized ryanodine receptors and a regulator of ER calcium homeostasis, prevents cell death in neural progenitor cells derived from induced pluripotent stem cells (iPSCs) of a Wolfram syndrome patient [10].

In this study, we analyzed the developing palate of *Ick*-mutant embryos and found that abnormal SHH signaling is a major pathological mechanism that leads to the cleft palate in the presence of ICK dysfunction. In addition, we sought to rescue the cleft palate of *Ick*-mutant mice via pharmacological activation of SHH signaling using a small molecule SHH pathway agonist (SAG). Intriguingly, we observed that treatment of pregnant mice with SAG rescued multiple congenital defects, including cleft palate, in the *Ick*-mutant embryos. These results provide *in vivo* evidence that SHH signaling is the primary cause of abnormal craniofacial developmental processes in ECO syndrome and further deepen our understanding of the pathogenesis of human genetic ciliopathies, supporting the development of therapeutic measures to alleviate congenital abnormalities caused by gene mutations.

2. Materials and Methods

2.1. Mice and SAG treatment

Mice carrying a knockout first allele of the *Ick* gene ($Ick^{tm1a/tm1a}$) were previously described [4]. $Ick^{tm1a/+}$ mice were housed in a specific-pathogen-free animal facility with constant temperature and humidity and ad libitum access to food and water. The embryos were obtained from time-mated pregnant mice. The day that a vaginal plug was confirmed was designated as embryonic day (E) 0.5. SAG was injected intraperitoneally into pregnant mice (20 mg/kg), and the embryos were harvested between E12.5 and E18.5 for analysis. All animal protocols were approved by the Institutional Animal Care and Use Committee at Yonsei University College of Medicine.

2.2. Histology and in situ hybridization

For histological analysis and *in situ* hybridization, embryos were fixed in 4% paraformaldehyde overnight, mounted in OCT compound (Tissue-Tek; Tokyo, Japan), and sectioned at a thickness of 12 μm onto Superfrost Plus slides (Tissue-Tek; Tokyo, Japan) using a cryostat (Thermo Scientific; Massachusetts, USA). Hematoxylin and eosin (H&E) staining as well as section and whole-mount *in situ* hybridization were performed as described previously [4, 11]. Antisense RNA probes for *Shh, Ptch1* [11], *Gli1* [12], *Smo* (+2066-+2980, NM_176996.4), and *Foxf1* (+588-+1434, NM_010426.2) were labeled with digoxigenin. All histology and *in situ* hybridization figures are representative of at least three different samples in two or more independent experiments.

2.3. Scanning electron microscopy

For scanning electron microscopy, palates of E12.5 $Ick^{tm1a/+}$ and $Ick^{tm1a/tm1a}$ embryos were isolated and fixed with 2.5% glutaraldehyde and 2% paraformaldehyde in 0.1 M sodium cacodylate buffer (pH 7.4) at 4 °C overnight. The specimens were washed three times for 30 min in 0.1 M sodium cacodylate buffer (pH 7.4). Then the

specimens were post-fixed with 1% osmium tetroxide at 4 °C for 1 h and immersed in saturated thiocarbohydrazide at room temperature for 20 min. Next, the specimens were dehydrated using a graded ethanol series, dried using a critical point dryer (Leica EM CPD300; Solms, Germany), affixed on a stub, and coated with platinum to a thickness of 20–30 nm using a sputter coater (E1030; Hitachi, Tokyo Japan). Lastly, the platinum-coated specimens were mounted on a stub holder and imaged using a Schottky emission scanning electron microscope (JSM 7001F, JEOL, Tokyo, Japan). Five different specimens were examined for SEM images.

2.4. Cell proliferation and cell death assays

Cell proliferation and cell death assays were performed as previously described [11]. For the cell proliferation assay, 5-ethynyl-2′-deoxyuridine (EdU; Invitrogen, Massachusetts, USA) was injected intraperitoneally into a pregnant female mouse at E12.5 at a concentration of 10 mg/g body weight. Embryos were harvested and fixed in 4% paraformaldehyde in 1 × PBS overnight at 4 °C. Embryos were then mounted and frozen in OCT compound (Tissue-Tek; Tokyo, Japan) and sectioned at a thickness of 12 μm onto Superfrost Plus slides (Tissue-Tek; Tokyo, Japan) using a cryostat (Thermo Scientific; Massachusetts, USA). EdU-labeled cells were identified using the Click-IT EdU imaging Alexa Fluor 488 Kit (Invitrogen; Massachusetts, USA). 4′,6-diamidino-2-phenylindole (DAPI) was used for nuclear staining. For the cell death assay, apoptotic cells were detected using the ApopTag Plus Peroxidase *In Situ* Apoptosis Detection Kit (S7101, Millipore; Massachusetts, USA), which detects apoptotic cells by labeling DNA strand breaks via the indirect TUNEL method. Three different specimens were examined for cell proliferation and TUNEL assays.

2.5. Quantitative real-time polymerase chain reaction (qPCR)

Palate tissues from E12.5 $Ick^{tm1a/+}$ and $Ick^{tm1a/tm1a}$ embryos were dissected in cold DEPC-treated PBS, followed by RNA isolation with the Trizol reagent (Thermo Fisher Scientific, USA) according to the manufacturer's instructions. cDNA synthesis was performed using PrimeScript™ 1st strand cDNA Synthesis Kit (TaKaRa, Japan). qPCR was performed using the TB Green™ Premix Ex Taq™ (TaKaRa, Japan) and an A28132 real-time PCR instrument system (Thermo Fisher Scientific, USA). The primer sequences of the genes are as follows: *Ptch1*, 5′-TGTCTGGAGTCCGGATGG-3′ and 5′-TGATTGTGGAAGCCACAGAAAA-3′; *Gli1*, 5′-GGTGCTGCCTATAGCCAGTGTCCT-3′ and 5′-GTGCCAATCCGGTGGAGTCAGACCC-3′; *Smoothened*, 5′-CTCGGGCAAGACATCCTATTT-3′ and 5′-ACTCACGGAGTCTCCATCTAC-3′; *GAPDH*, 5′-CCTGTTGCTGTAGCCGTATT-3′ and 5′-AACAGCAACTCCCACTCTTC-3′. Student's *t*-tests were used to determine statistical significance. $P < 0.05$ was considered as significant.

2.6. Palate explant culture and immunohistochemistry for Ki67

Palate explant culture was performed as previously described [13]. Briefly, tissues containing palatal shelves were dissected from E13.5 embryos and placed on filter Trowell-type organ cultures. Palatal shelves were brought into contact and cultured in DMEM/F12 (Gibco; Massachusetts, USA) supplemented with 20 μg/ml ascorbic acid (Sigma; Missouri, USA) and 1% penicillin/streptomycin without fetal bovine serum at 37 °C in a CO_2 chamber. The palatal explants were incubated for 48 h to conduct *in vitro* palatal fusion assay (Fig. 4) or for 24 h to examine changes in gene expression or cell proliferation (Fig. 7). The culture medium containing 200 nM SAG or DMSO was replaced every 24 h. The cultured palate tissues were fixed in 4% paraformaldehyde, embedded in OCT compound, and sectioned at a thickness of 12 μm onto Superfrost Plus slides (Tissue-Tek; Tokyo, Japan). Sections were incubated with Ki67 antibody (Thermo Scientific; Massachusetts, USA) at 4 °C overnight. After washing with PBST, the specimens were sequentially incubated with secondary antibody and streptavidin peroxidase. The Ki67-positive cells were visualized using a diaminobenzidine reagent kit (Invitrogen; Massachusetts, USA) and the sections were counterstained with hematoxylin. Palate explant culture experiments were performed using four specimens in each analysis, which were repeated three times.

2.7. Quantitation, measurement, and statistical analysis

EdU-positive cells were counted in the epithelium and mesenchyme of palatal shelves of control and mutant embryos. The genotypes were blinded to the investigators conducting the cell counting. Cell proliferation rate was calculated as a percentage of EdU-positive cells per DAPI-positive cells. Lengths of primary cilia were measured from SEM images of E12.5 embryos, and distances between right and left palatal shelves were measured from images of E18.5 embryos using the ImageJ software. All cell counting and length measurement were conducted in at least three different embryos for each genotype. Two-tailed, unpaired Student's *t*-tests were used to determine statistical significance. $P < 0.05$ was considered as significant. Data are shown as means ± s.d.

3. Results

3.1. ICK deficiency caused cleft palate and abnormally elongated primary cilia in the developing palate of mice

To investigate the role of ICK in palate development, we analyzed the palates of $Ick^{tm1a/tm1a}$ embryos at E18.5 (Fig. 1). Gross morphological analysis revealed a completely divided palate along the anteroposterior axis including the entire primary and secondary palates in $Ick^{tm1a/tm1a}$ mice compared to the correctly formed palate in $Ick^{tm1a/+}$ control mice (Fig. 1A and E). Histologically, the palatal shelves from the left and right sides were fused at the midline along the anteroposterior axis in $Ick^{tm1a/+}$ heterozygous control mice (Fig. 1B–D). In contrast, the palatal shelves of $Ick^{tm1a/tm1a}$ mice remained separated, resulting in a complete cleft palate (Fig. 1F–H). The palatal shelves were elevated to a horizontal position in the anterior region (Fig. 1F) but not in the middle and posterior regions in $Ick^{tm1a/tm1a}$ mice (Fig. 1G–H). The cleft palate phenotype was completely penetrant in $Ick^{tm1a/tm1a}$ mutant embryos ($n = 10/10$).

We further analyzed the developing palates at E12.5 before palatal fusion by scanning electron microscopy (Fig. 1I–P). The distance between the anterior palatal shelves in the $Ick^{tm1a/tm1a}$ mutants was wider than that in $Ick^{tm1a/+}$ control embryos (Fig. 1I, M, red arrows). Moreover, the formation of palatal rugae was evident in the palatal shelves of $Ick^{tm1a/+}$ control embryos; however, this structure was not present in $Ick^{tm1a/tm1a}$ mutants (Fig. 1I, J, M, N). The distance of the medial maxillary prominence that later develops into the lip was longer in $Ick^{tm1a/tm1a}$ embryos than in $Ick^{tm1a/+}$ embryos (Fig. 1K, O; black arrows). In addition, the surface of the primary palatal shelves that were derived from the medial nasal prominence were rugged in $Ick^{tm1a/tm1a}$ mutants (Fig. 1I, K, L, M, O, P).

It has previously been reported that ICK plays a critical role in the regulation of primary cilia length during limb and lung development [4, 5]. Consistent with previous reports, the lengths of primary cilia in the palatal shelves were significantly elongated and the morphology of the ciliary tip region bulged in $Ick^{tm1a/tm1a}$ mutant embryos compared with $Ick^{tm1a/+}$ control embryos (Fig. 1J′, L′,

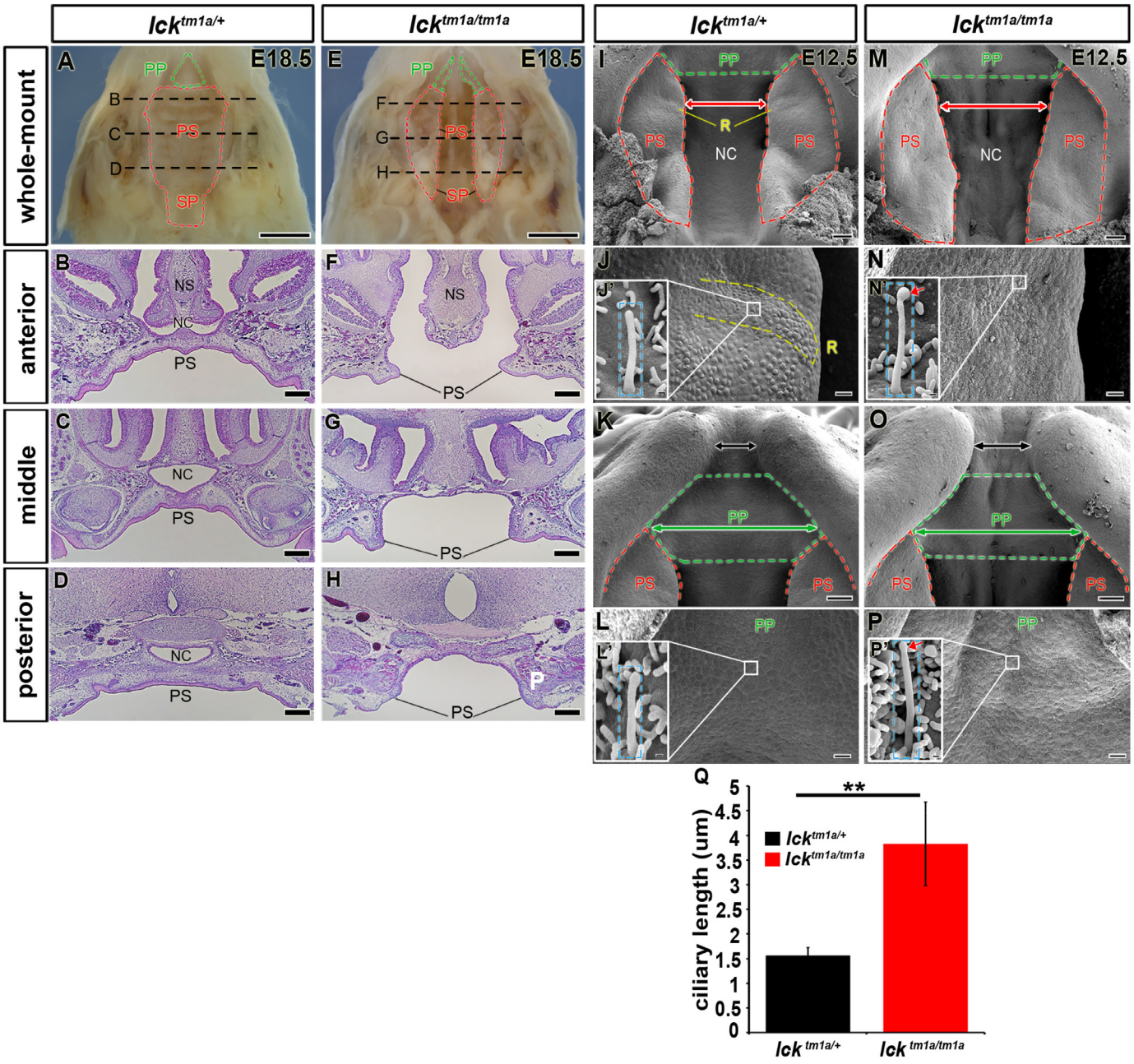

Fig. 1. Defects of palates and primary cilia in *Ick*-deficient mice. (A) An $Ick^{tm1a/+}$ embryo showing an intact palate at E18.5. (B–D) Hematoxylin and Eosin staining showing normal palate from the anterior to the posterior regions in $Ick^{tm1a/+}$ embryo. (E) An $Ick^{tm1a/tm1a}$ embryo showing a cleft palate at E18.5. (F-H) Hematoxylin and Eosin staining showing separation of palatal shelves on either side in $Ick^{tm1a/tm1a}$ embryo at E18.5. (I-P) Scanning electron microscopy analysis of developing palates in $Ick^{tm1a/+}$ and $Ick^{tm1a/tm1a}$ embryos at E12.5. (I, M) Overall view of the developing palates at E12.5. (J, N) High magnification of palatal rugae in the anterior region of the developing palate in $Ick^{tm1a/+}$ and $Ick^{tm1a/tm1a}$ mice. (K, O) Morphology of primary palate and upper lip in $Ick^{tm1a/+}$ and $Ick^{tm1a/tm1a}$ mice. (L, P) Primary cilia of the palatal epithelium in $Ick^{tm1a/+}$ and $Ick^{tm1a/tm1a}$ mice. (Q) Lengths of primary cilia in the developing palates of $Ick^{tm1a/tm1a}$ embryos were significantly elongated compared with those of $Ick^{tm1a/+}$ embryos. Data are shown as mean ± s.d. $^{**}p < 0.01$. PP, primary palate; PS, palatal shelf; NC, nasal cavity; and R, rugae. Green dotted line, primary palate; red two-way arrows, distance between left and right palatal shelves; red dotted line, secondary palate; blue dotted box, primary cilia; red arrow, bulged tip of primary cilia; yellow dotted line, palatal rugae; and black dotted line, section plane. Scale bars, A, E: 1 mm; B-D, F-H, I, K, M, O: 100 μm; J, L, N, P: 20 μm; J′, L′, N′, P′: 20 nm.

N′, P′, Q). These results suggest that ICK plays an essential role in the regulation of the length of primary cilia for normal palatal development.

3.2. ICK deficiency resulted in disrupted SHH signaling in the developing palate of mice

The observed, abnormally elongated primary cilia prompted us to examine SHH signaling activity in the developing palate because primary cilia act as essential signaling centers for SHH signal transduction, which is crucial for animal development and homeostasis [14]. In the developing palate, *Shh* is expressed in the ridges of developing palatal rugae and positively regulates expression of Patched 1 (*Ptch1*), GLI-Kruppel family member GLI1 (*Gli1*), and Forkhead box F1 (*Foxf1*) [6, 15]. We examined these genes using whole-mount and section *in situ* hybridization in E12.5 developing palates of mouse embryos (Fig. 2). Consistent with previous reports, two ridges of developing rugae expressed *Shh* and its tar-

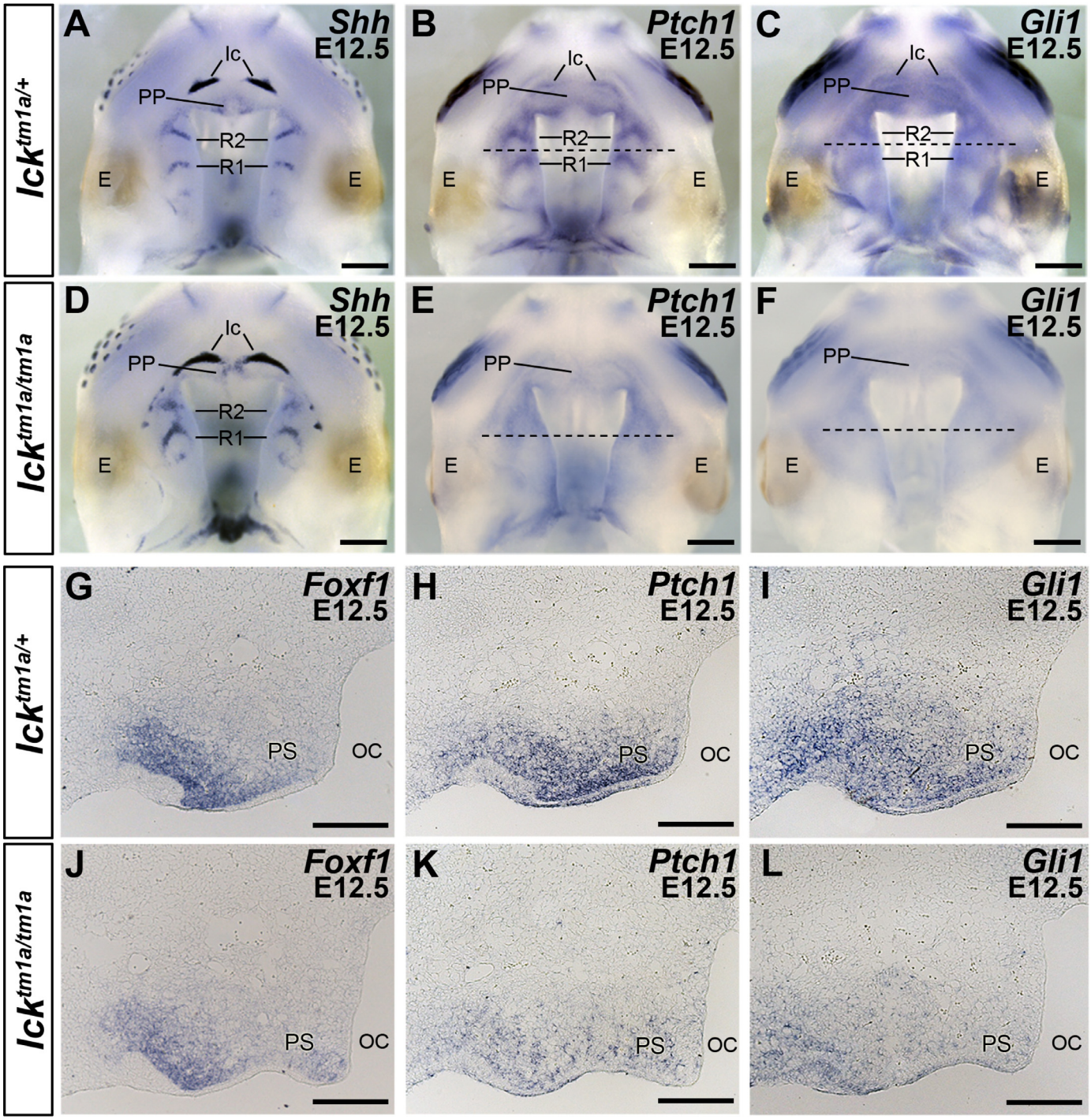

Fig. 2. Gene expression analyses in the developing palate in *Ick*-deficient mice. (A–F) Whole mount *in situ* hybridization results showing expression of *Shh* (A, D), *Ptch1* (B, E), and *Gli1* (C, F) in $Ick^{tm1a/+}$ and $Ick^{tm1a/tm1a}$ embryos at E12.5. (G–L) Section *in situ* hybridization results showing expression of *Foxf1* (G, J), *Ptch1* (H, K), and *Gli1* (I, L) in the palatal mesenchyme and epithelium in $Ick^{tm1a/+}$ and $Ick^{tm1a/tm1a}$ embryos. Ic, incisor; R, palatal rugae; PP, primary palate; PS, palatal shelf; SP, soft palate; OC, oral cavity. black dotted line, section plane. Scale bars, A–F: 500 μm; G–L: 200 μm.

get genes *Ptch1* and *Gli1* in each palatal shelf of $Ick^{tm1a/+}$ control embryos (Fig. 2A–C and Fig. S1). In $Ick^{tm1a/tm1a}$ mutant embryos, expression levels of *Shh* were generally unaffected but its expression domains were slightly expanded in less clearly defined rugae compared with those of $Ick^{tm1a/+}$ embryos (Fig. 2D). Interestingly, expression of *Ptch1* and *Gli1* was greatly reduced and appeared diffuse without a distinct palatal rugae pattern in $Ick^{tm1a/tm1a}$ embryos (Fig. 2E and F and Fig. S1). *In situ* hybridization of tissue sections confirmed these findings, showing that expression of *Ptch1* and *Gli1* was downregulated in the palatal mesenchyme and epithelium in $Ick^{tm1a/tm1a}$ embryos at E12.5 compared to control embryos (Fig. 2H, I, K, L). *Foxf1* was also downregulated in the mesenchyme of the developing palatal shelf (Fig. 2G and J). These results suggest that ICK is essential for the regulation of ciliary length and subsequent normal transduction of SHH signaling in the developing palate.

3.3. Cleft palate in Ick-deficient mice was caused by impaired palatal growth that resulted from decreased cell proliferation

It has been shown that SHH signaling contributes to palatal outgrowth by promoting cell proliferation [6]. Therefore, we determined whether the cleft palate in *Ick*$^{tm1a/tm1a}$ mutants results from insufficient extension of palatal shelves toward the midline due to decreased cell proliferation. Cell proliferation was analyzed by counting the number of cells in the developing palate that had incorporated EdU at E12.5. The *Ick*$^{tm1a/tm1a}$ embryos exhibited a significant reduction of cell proliferation in the palatal mesenchyme compared with *Ick*$^{tm1a/+}$ control embryos (Fig. 3A, A-a, B, B-a, E). Interestingly, the number of EdU-positive cells was significantly decreased in the palatal epithelium on the oral side (Fig. 3A-b, B-b, E) but not in the nasal side epithelium (Fig. 3A-c, B-c, E). Since the oral side but not nasal side epithelium expresses *Ptch1* in *Ick*$^{tm1a/+}$ embryos and this *Ptch1* expression was dramatically reduced in *Ick*$^{tm1a/tm1a}$ embryos (Fig. 2H, K), the decrease of EdU-positive cells in the palatal epithelium appears to be closely related with reduced SHH activity. In contrast, TUNEL-positive apoptotic cells were not detected in the palatal mesenchyme or epithelium in either *Ick*$^{tm1a/+}$ or *Ick*$^{tm1a/tm1a}$ embryos (Fig. 3C and D). These results suggest that *Ick* deficiency causes decreased cell proliferation in *Ptch1*-positive regions in the developing palate.

The defective fusion between bilateral palatal shelves is one of the main causes of cleft palate [16]. Primary cilia have also been implicated in mediating signaling pathways important for palatal fusion including Wnt and transforming growth factor beta (TGFβ) signaling [14, 17]. To test whether the cleft palate in *Ick*$^{tm1a/tm1a}$ embryos is also attributed to disruption of other signaling pathways important for palatal fusion, we performed *ex vivo* palatal fusion analysis. Palatal fusion involves the formation of the midline epithelial seam (MES) and its subsequent degeneration, leading to palatal mesenchymal confluence [16]. A pair of palatal shelves dissected from E13.5 embryos were placed facing one another in an explant culture system (Fig. 4A–C). After 48 h in culture, we observed complete fusion between the palatal shelves, assessed by the complete degeneration of MES, in both *Ick*$^{tm1a/+}$ and *Ick*$^{tm1a/tm1a}$ embryos (Fig. 4D–E; dotted rectangles). Together, these results suggest that the cleft palate in *Ick*$^{tm1a/tm1a}$ animals is caused by defective palatal outgrowth resulting from decreased cell proliferation and not by defective fusion of the MES.

3.4. Timely activation of SHH signaling by SAG rescued the developmental defects in Ick$^{tm1a/tm1a}$ mutant embryos

Our analyses indicated that the lack of ICK function in the developing palate causes defective cilia and a reduction of SHH signaling, leading to a decrease of cell proliferation, a subsequent failure of palatal outgrowth, and ultimately a cleft palate. Thus, we hypothesized that activation of SHH signaling during the critical developmental period for palate outgrowth could rescue the cleft palate in *Ick*$^{tm1a/tm1a}$ embryos. We tested this idea by treating *Ick*$^{tm1a/tm1a}$ embryos with a synthetic agonist of the SHH pathway, SAG [18]. SAG is able to cross the gut, placenta, and blood-brain barrier [19–21] and constitutively activate SHH signaling by directly binding to the SHH signaling transducer Smoothened (Smo) [19, 22].

Palatal primordia emerge from the maxillary prominence and rapidly grow bilaterally around E11.0 and E11.5 [23]. Thus, we injected DMSO or SAG intraperitoneally into pregnant mice at E10.5, E11.25, or E13.5 and analyzed the treated embryos at E18.5 (Fig. 5A). Interestingly, we observed rescue of cleft palate in *Ick*$^{tm1a/tm1a}$ embryos that were treated with SAG at E10.5 and E11.25 but not at E13.5, and treatment at E11.25 resulted in the best rescue efficiency (Fig. 5F). Embryos treated with SAG at E10.5 suffered from other developmental defects, such as polydactyly, reduced head size, cleft lip, edema, and spina bifida (Fig. 5B–D), consistent with previous reports that administration of SAG in early gestation causes preaxial polydactyly in mice [24]. Embryos treated with SAG at E11.25 showed generally better overall morphology with a complete fusion of the palate when rescued (Fig. 5E, O). These results suggest that the outcome of SAG treatment during the prenatal stage is dependent on the developmental stage of treatment administration. Histological analysis showed that the secondary palate was well fused from anterior to posterior and that the nasal cavity and oral cavity were well separated in *Ick*$^{tm1a/tm1a}$ embryos treated with SAG but not with DMSO at E11.25 (Fig. 5G–R). Together, these results suggest that timely administration of SAG can rescue the cleft palate in *lck*-mutant mice, and this timing is correlated with the developmental timing of innate Shh signaling.

Our results showed that the extent of phenotypic recovery by SAG treatment in E11.25 *Ick*$^{tm1a/tm1a}$ embryos was variable (Fig. 5F). The rescue phenotypes could be divided into three categories: completely rescued (6/16, 37.5%), partially rescued (3/16, 18.75%), and not rescued (7/16, 43.75%; Fig. S2). The palates of partially rescued embryos were fused, but the palatal rugae patterning was irregular compared with those of completely rescued embryos (Fig. S2B–C). In contrast, the palates of the embryos that were not rescued were not fused, displaying a complete cleft palate (Fig. S2D). Comparing the SAG-treated mutants that were not rescued with DMSO-treated mutants, we noticed that the distance of the anterior palatal shelves of SAG-treated mutants was slightly, yet significantly, closer compared with those of DMSO-treated mutant embryos (Fig. S3G). In addition, the palates of the SAG-treated mutants exhibited more regular rugae patterning compared with those of DMSO-treated mutant embryos (Fig. S3A–F; 4/7, 57.1%).

An inactivation mutation in the human *ICK* gene shows multiple visceral abnormalities, including a hypoplastic ileum [3]. Our *Ick*-mutant mouse model also displayed defects in gastrointestinal development with short underdeveloped small and large intestines (Fig. S4E–F) and imperforate rectum (Fig. S4G). Since SAG was systemically applied in our experimental design, we examined the effect of SAG on the intestinal defects in the *Ick*$^{tm1a/tm1a}$ embryos. Interestingly, the intestines of SAG-treated mutant embryos were elongated compared with those of DMSO-treated embryos (Fig. S4; 2/11, 18.18%). Rescue of the imperforate rectum was also observed in SAG-treated *Ick*$^{tm1a/tm1a}$ embryos (Fig. S4; 2/11, 18.18%).

3.5. SAG treatment resulted in increased SHH signaling and cell proliferation in the developing palate of Ick$^{tm1a/tm1a}$ embryos

The restoration of the cleft palate by SAG treatment in *Ick*$^{tm1a/tm1a}$ embryos prompted us to examine whether SAG indeed activates SHH signaling in the developing palate of *Ick*$^{tm1a/tm1a}$ mutants. We treated *Ick*$^{tm1a/+}$ and *Ick*$^{tm1a/tm1a}$ pregnant female mice with DMSO or SAG at E11.5 and examined expression patterns of SHH target genes such as *Ptch1* and *Gli1* by *in situ* hybridization and quantitative real-time PCR (qPCR). *In situ* hybridization results showed that *Ptch1* and *Gli1* expression was greatly increased in SAG-treated embryos compared to DMSO-treated embryos in both *Ick*$^{tm1a/+}$ and *Ick*$^{tm1a/tm1a}$ mice (Fig. 6A–H). In contrast, *Smo* expression was similar between SAG- and DMSO-treated embryos in both genotypes (Fig. 6I–L). qPCR results also showed that mRNA levels of *Ptch1* and *Gli1*, but not *Smo*, were significantly increased in SAG-treated embryos compared to DMSO-treated embryos in both *Ick*$^{tm1a/+}$ and *Ick*$^{tm1a/tm1a}$ mice (Fig. 6M–O). Interestingly, expression levels of *Ptch1* and *Gli1* of SAG-treated *Ick*$^{tm1a/tm1a}$ embryos were not significantly different from those of DMSO-treated *Ick*$^{tm1a/+}$ embryos (Fig. 6M and N), suggesting that SAG treatment

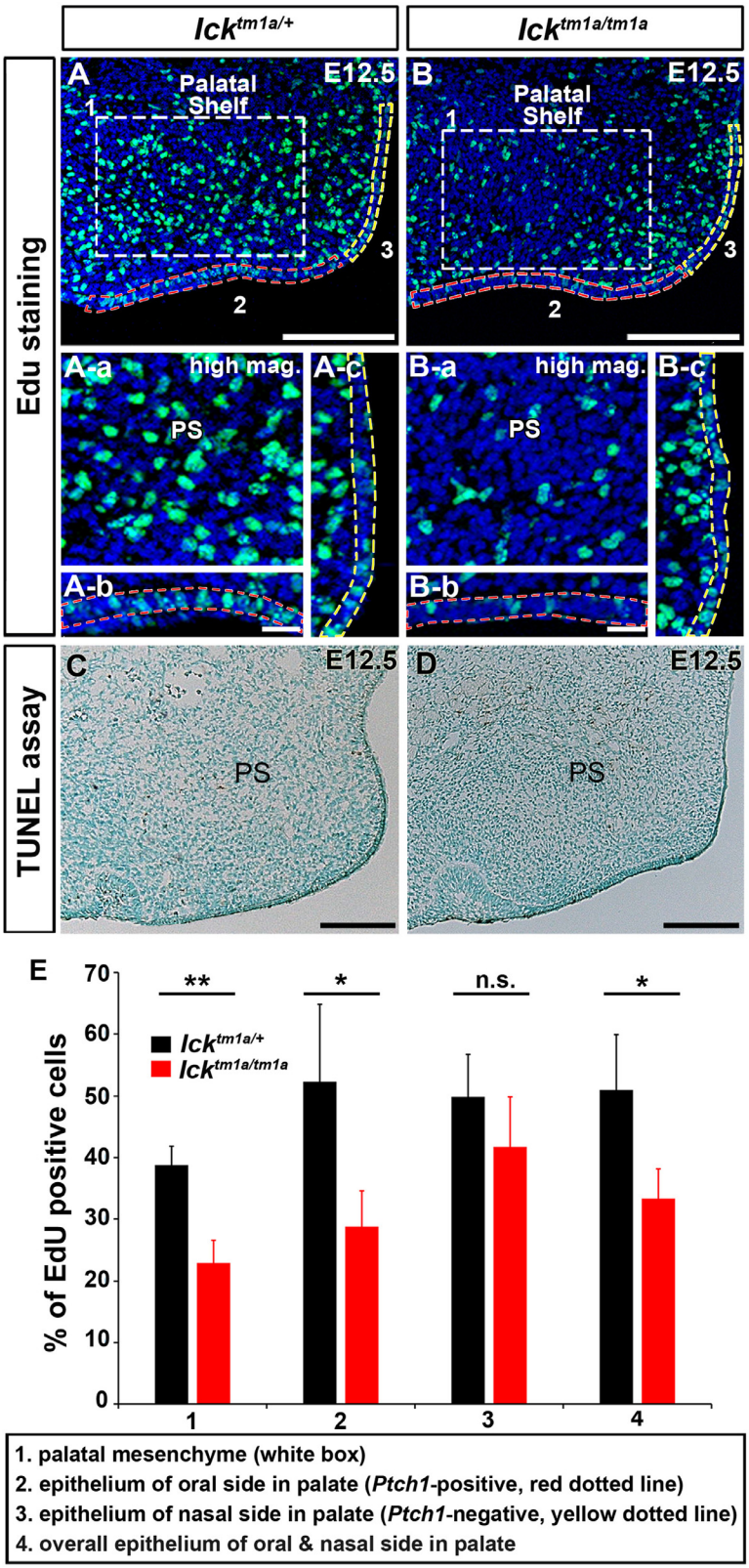

Fig. 3. Analyses of cell proliferation and cell death in the developing palates of *Ick*-deficient embryos at E12.5. (A, B) EdU-positive cells in the developing palates of $Ick^{tm1a/+}$ and $Ick^{tm1a/+}$ embryos. Higher magnification images of EdU assay for palatal shelves (A-a and B-a), oral side palatal epithelium (A-b and B-b), and nasal side palatal epithelium (A-c and B-c). (C, D) TUNEL-positive cells in the developing palates of the $Ick^{tm1a/+}$ and $Ick^{tm1a/tm1a}$ embryos. (E) Percentages of EdU-positive cells in the defined regions of the palatal shelves of $Ick^{tm1a/+}$ and $Ick^{tm1a/+}$ embryos. PS, palatal shelf; white dotted line, counted total cells and EdU-positive cells in the palatal mesenchyme; red dotted line, the palatal epithelium on the oral side; and yellow dotted line, the palatal epithelium on the nasal side. Error bars indicate standard deviation. Data are shown as mean ± s.d. $^{*}p < 0.05$, $^{**}p < 0.01$. n.s., not significant. Scale bars, A-D: 200 μm; A-a to B-c: 20 μm.

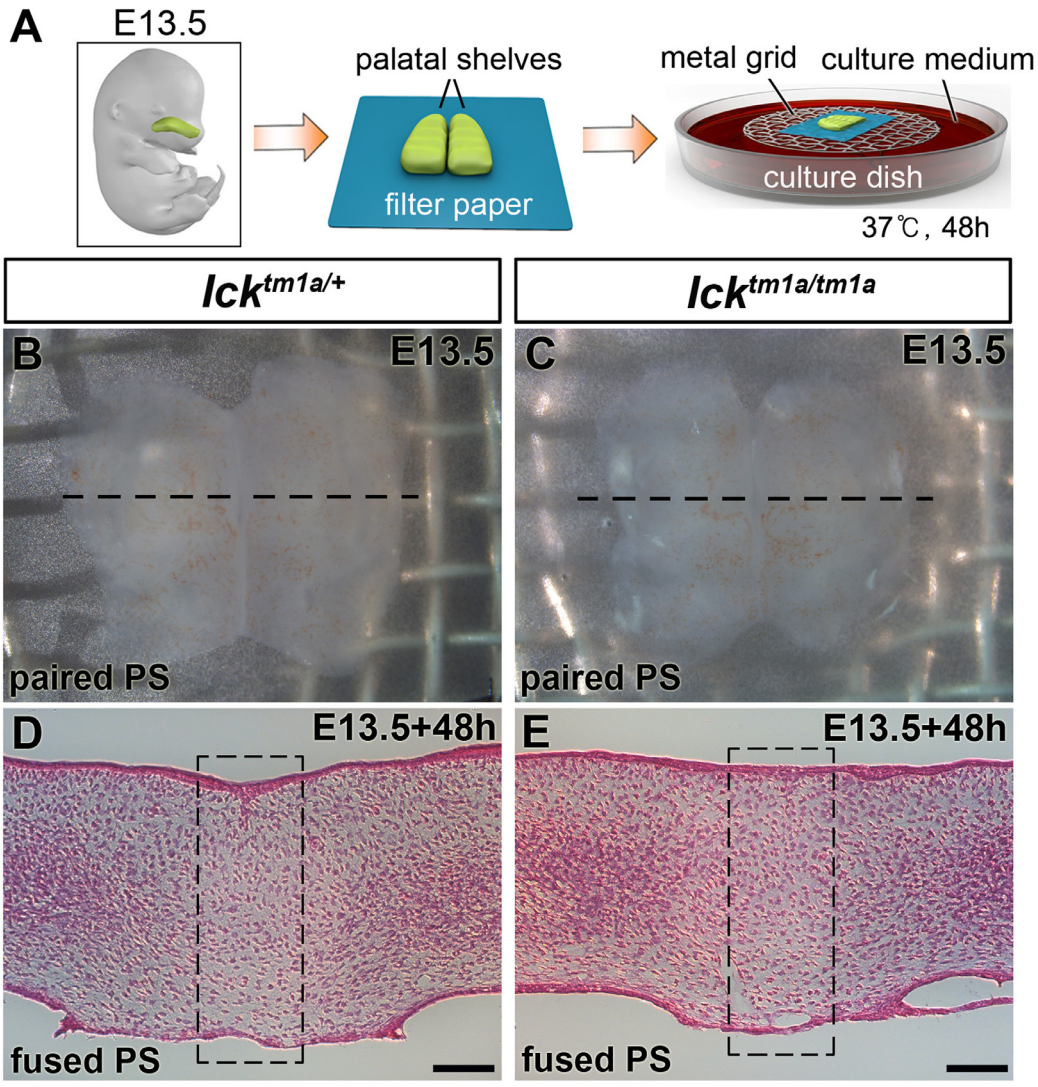

Fig. 4. *In vitro* palatal fusion assay in *Ick*-deficient embryos. (A) Diagrams showing the *in vitro* organ culture system for analysis of the paired secondary palatal shelves. (B, C) Oral-side view of contacted palatal shelves from the $Ick^{tm1a/+}$ and $Ick^{tm1a/tm1a}$ embryos. (D, E) H&E staining of contacted palatal shelves from the $Ick^{tm1a/+}$ and $Ick^{tm1a/tm1a}$ embryos after 48h in organ culture. Scale bars, D, E: 50 μm.

activates SHH signaling in *Ick*-deficient embryos to comparable levels to control embryos.

We further examined SAG effects on SHH signaling and cell proliferation using palatal organ culture (Fig. 7). We administered SAG to the culture medium of the palate organ culture for 24 h. Histological analysis showed that unlike 48 h cultured palate explants (Fig. 4), the palatal fusion was still undergoing and the MES remained in both $Ick^{tm1a/+}$ and $Ick^{tm1a/tm1a}$ embryos (Fig. 6A, E, black dotted circles). *In situ* hybridization analysis showed that the expression levels of *Ptch1* and *Gli1* were upregulated in response to SAG treatment in the palates of $Ick^{tm1a/tm1a}$ mutant embryos compared to those of DMSO-treated $Ick^{tm1a/+}$ embryos (Fig. 7B, C, F, G). In addition, SAG treatment increased the number of Ki67-positive cells in the developing palate of $Ick^{tm1a/tm1a}$ mutant embryos (Fig. 7D and H). These results suggest that the Smo agonist activates SHH signaling in ciliary mutants and promotes cell proliferation in palate organ culture.

4. Discussion

In this study, we studied the mechanism by which ICK deficiency causes developmental defects in an *Ick*-mutant mouse model with focus on the cleft palate phenotype, which is one of the main clinical features of ECO syndrome. We found that decreased SHH signaling caused by abnormal regulation of ciliary length is a major cause of cleft palate in *Ick*-mutant mice (Fig. 8). In addition, we demonstrated that proper temporal modulation of SHH signaling with a Smo agonist rescues the cleft palate in *Ick* mutants by activating SHH signaling, which restores palatal cell proliferation and palatal-shelf outgrowth (Fig. 8). These results suggest that timely modulation of key developmental signaling pathways using small chemical compounds offers therapeutic potential to prevent congenital defects in genetic diseases, such as ciliopathies.

Mammalian palatogenesis is a multi-step process in which nasal and maxillary prominences expand to develop into the primary and secondary palatal shelves, respectively, which then fuse together to form a roof structure that separates the oral and nasal cavities [16]. Outgrowth of the lateral palatal shelves toward the medial direction is a critical step for an intact palate. Palatal-shelf outgrowth has been associated with several signaling pathways, including SHH, fibroblast growth factors (FGFs), and bone morphogenic proteins (BMPs). Crosstalk between SHH signaling in the early palatal epithelium and FGF and BMP signaling in the under-

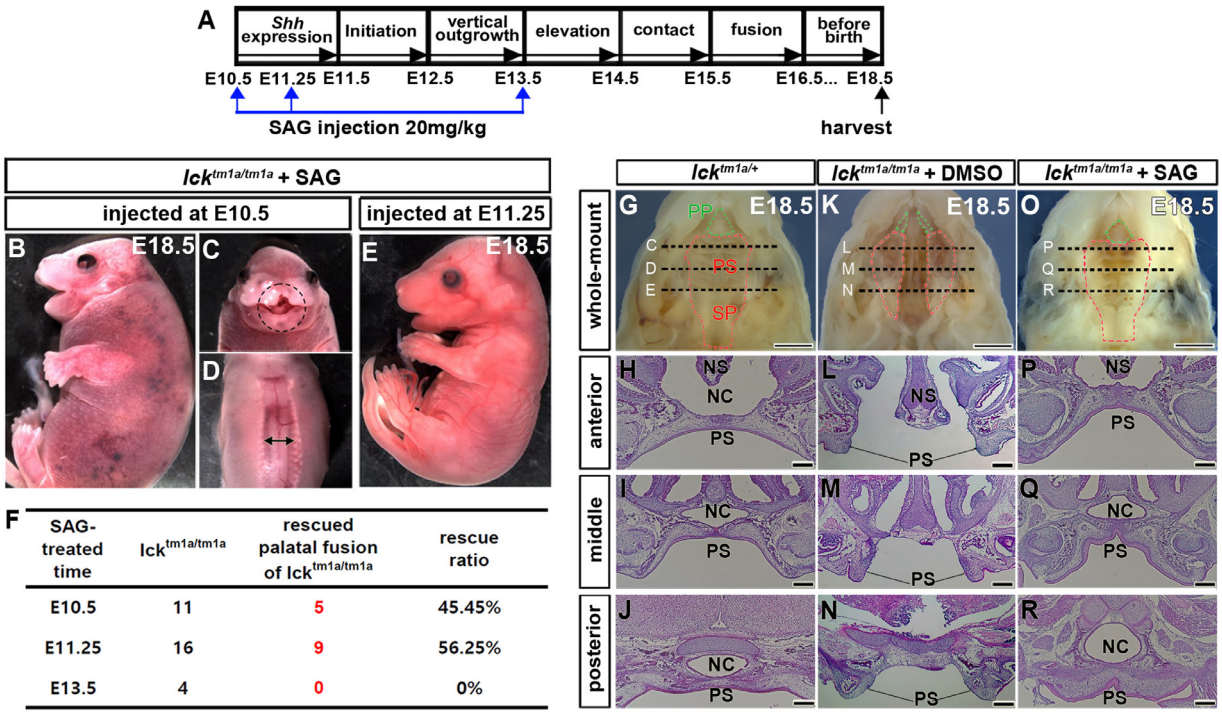

Fig. 5. Restoration of cleft palate in the *Ick*-deficient embryos after SAG treatment. (A) Experimental design for the controlled delivery of SAG during palatogenesis. Blue arrows indicate injection day and vertical black arrow indicate tissue harvest day. (B-D) $Ick^{tm1a/tm1a}$ mice treated with SAG at E10.5 exhibit hypoplastic forebrain, polydactyly, and overgrown skin (B), cleft lip (C), and unclosed neural tube (D) at E18.5. (E) Morphology of E18.5 $Ick^{tm1a/tm1a}$ mice treated with SAG at E11.25. (F) Rescue rate of cleft palate in the $Ick^{tm1a/tm1a}$ mice at E18.5 according to time of SAG treatment. (G, K, O) Oral-side view of the palate in the $Ick^{tm1a/+}$ and DMSO- or SAG-treated $Ick^{tm1a/tm1a}$ embryos at E18.5. (H-J, L-N, P-R) Histological analysis of the palatal shelves from the anterior to posterior region of E18.5 $Ick^{tm1a/+}$ and $Ick^{tm1a/tm1a}$ mice treated with DMSO or SAG at E11.25. PP, primary palate; PS, palatal shelf; SP, soft palate; NC, nasal cavity; NS, nasal septum, green dotted line, primary palate; red dotted line, secondary palate. Scale bars, G, K: 1 mm; H–J, L–N: 100 μm.

lying mesenchyme drives palatal cell proliferation and palatal-shelf outgrowth [6, 25]. Perturbation of any of these signaling pathways can disrupt palatal growth and fusion, resulting in cleft palate.

Although cleft palate is one of the main features observed in ECO syndrome patients, its molecular etiology has not been directly examined [1, 2]. Our results demonstrate that the initial development of bilateral palatal shelves is normal in mouse models for ECO syndrome, yet the palatal shelves fail to grow and remain separated on both sides (Fig. 1). This phenotype closely resembles that of *Shh*-deficient mice, which exhibit initial development of palatal shelves and then defective palatal outgrowth and fusion [6, 15]. Consistent with these results, downstream SHH signaling targets, such as *Ptch1, Gli1*, and *Foxf1,* were greatly downregulated in the palatal epithelium and mesenchyme of *Ick*-deficient mice (Fig. 2). These results suggest that abnormal SHH signaling is a major pathological mechanism that underlies development of the cleft palate in ECO syndrome.

During palatogenesis, palatal shelves extensively proliferate to outgrow ventrally and then horizontally, and ultimately generate the fusion [16]. At the elongation stage, SHH promotes palatal cell proliferation through activation and maintenance of cell cycle regulators, such as cyclin D1 and cyclin D2 [6]. Consistent with these results, $Ick^{tm1a/tm1a}$ embryos, which have disrupted SHH signaling, showed significantly decreased cell proliferation in the palatal cells (Fig. 3). Interestingly, cell proliferation was impaired in the *Ptch1*-positive palatal mesenchyme and the palatal epithelium on the oral side but not in the *Ptch1*-negative palatal epithelium on the nasal side, indicating that impaired cell proliferation in *Ick*-deficient embryos is closely associated with SHH signaling.

Primary cilia in the presumptive palatal shelves of *Ick*-deficient mice were abnormally elongated, as shown in the developing limbs and lungs of the mutant mice (Fig. 1) [3, 4]. Previous studies demonstrated that ICK negatively regulates ciliary elongation by controlling axonemal microtubule stability or intraflagellar transport (IFT) velocity [26–29]. Thus, cleft palate in ECO syndrome is attributable to diminished SHH response in *Ptch1*-positive palatal cells due to the abnormally elongated primary cilia, which stems from increased cilia IFT kinetics or axonemal microtubule stability due to the lack of ICK function. Consistent with these results, intraflagellar transport 88 (*IFT88*), which is essential for the assembly and function of primary cilia, has been proposed to be a candidate gene for cleft palate in humans [30]. Since ciliogenesis and SHH signaling is disrupted in *Ift88* mutant embryos [30], abnormal SHH signaling appears to be a common mechanism leading to cleft palate in ciliopathies.

Besides SHH signaling, epithelial WNT signaling has been shown to regulate palatal fusion by regulating transforming growth factor beta (TGFβ) signaling [17]. Although primary cilia are proposed to mediate multiple signaling including WNT [14], our palatal fusion assay showed that the mechanisms controlling palatal fusion are intact in $Ick^{tm1a/tm1a}$-mutant embryos (Fig. 4). These results confirm the notions that SHH signaling is the main effector of ciliary function in palate development and that impaired SHH signaling is the major mechanism underlying cleft palate caused by the lack of ICK function. Although SHH signaling is known to be required for craniofacial development during early stages around E8 in mice [31], the development of maxillary prominence was relatively normal in the *Ick*-deficient mutants (Fig. 1), suggesting that mediation of SHH signaling by ICK-regulated ciliogenesis is required for normal palatogenesis after the formation of the maxillary prominence.

Consistent with these ideas, palatal defects in the $Ick^{tm1a/tm1a}$ embryos can be rescued through time-controlled delivery of the Smoothened agonist SAG (Fig. 5). Previously, in a mouse model

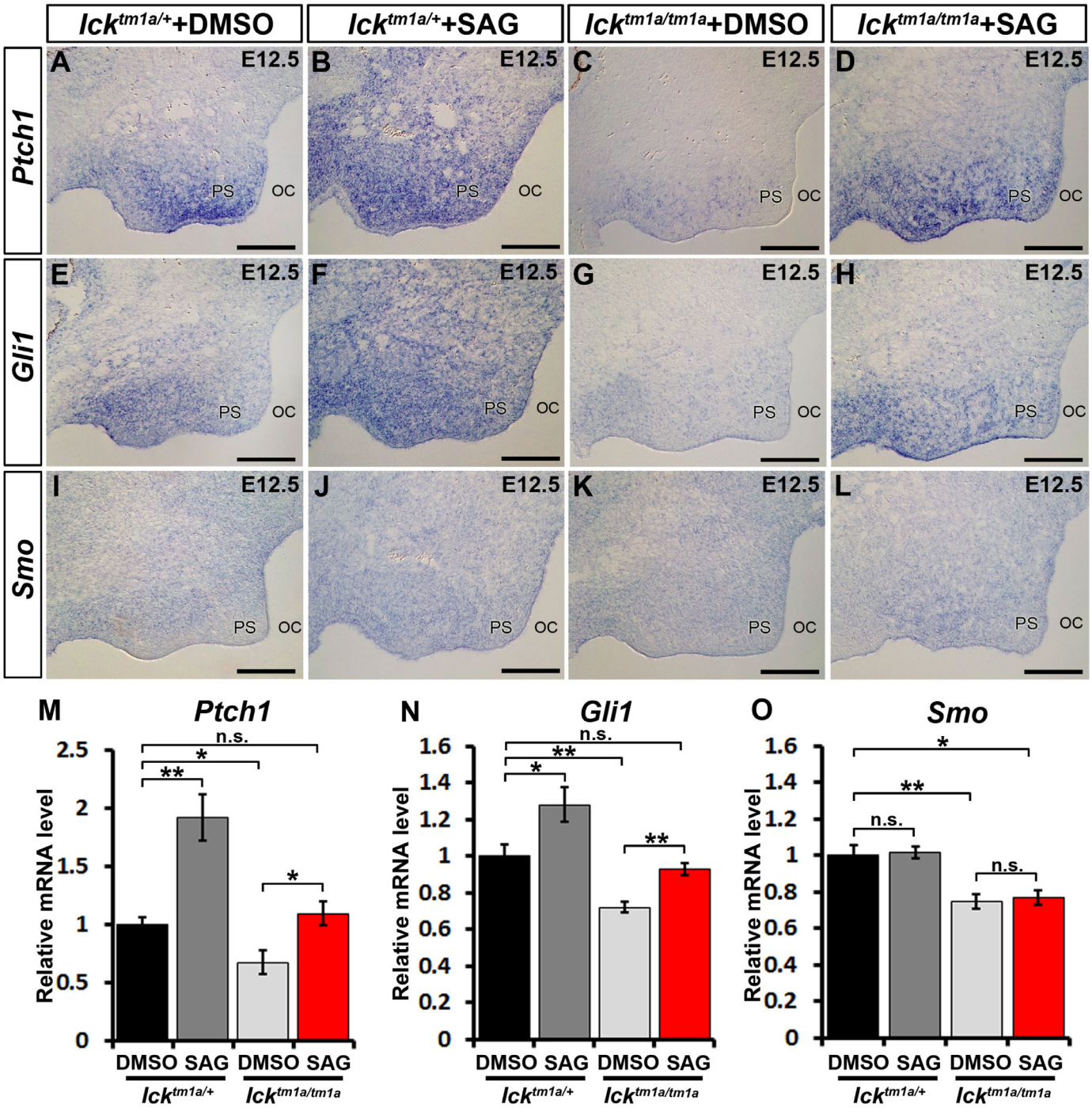

Fig. 6. Expression patterns of SHH target genes in SAG-treated *Ick*-deficient embryos. (A-L) Section *in situ* hybridization results showing expression patterns of *Ptch1* (A-D), *Gli1* (E-H), and *Smo* (I-L) in the palatal shelves of E12.5 $Ick^{tm1a/+}$ and $Ick^{tm1a/tm1a}$ treated with DMSO or SAG. (M-O) Quantitative real-time PCR results showing expression levels of *Ptch1* (M), *Gli1*(N), and *Smo* (O) in the palatal shelves of E12.5 $Ick^{tm1a/+}$ and $Ick^{tm1a/tm1a}$ treated with DMSO or SAG. PS, palatal shelf; OC, oral cavity. Scale bars, A-L: 200 μm. Data are shown as mean ± s.d.*$P < 0.05$, ** $P < 0.01$, *** $P < 0.001$, n.s., not significant

of Down syndrome (DS), SAG treatment was found to restore the morphology and function of the cerebellum as well as the function of the hippocampus [32]. Specifically, a single SAG treatment at birth in DS mice reversed the defects in cerebellar and hippocampus development and also improved behavior, learning, and memory. Similar with these findings, we observed that acute SAG treatment at a specific prenatal stage can overcome congenital palatal defects in ECO syndrome, raising the possibility of therapeutic potential for pharmacological intervention in congenital defects of genetic diseases.

Rescue of the cleft palate phenotype by SAG treatment confirms that abnormal SHH signaling is a primary mechanism underlying the palatal cleft in *Ick*-deficient mice; however, we observed considerable variability of the rescued phenotypes, depending on the timing of treatment. Furthermore, even SAG treatment at E11.25, which yielded the best rescue efficiency, restored the palatal fusion in only 56% (9/16) of the treated mutant embryos (Fig. 5). This variance may be due to ICK roles other than ciliary length regulation, and thus, SHH signaling may not be the sole pathway affected by ICK deficiency. Indeed, ICK has been shown to regulate

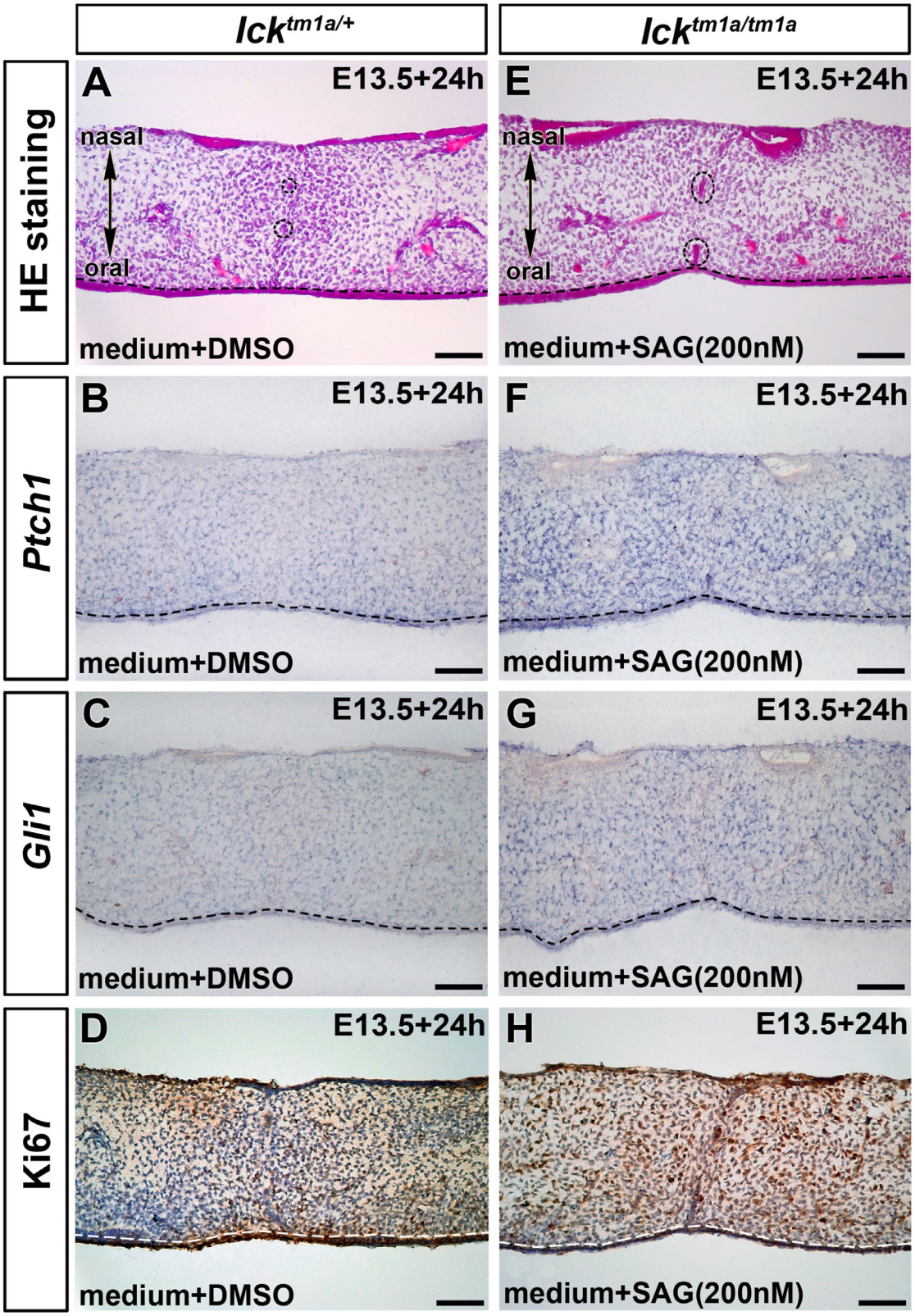

Fig. 7. Restoration of SHH signaling and cell proliferation in the SAG-treated *Ick*-deficient palate. (A, E) H&E staining showing the morphology of control $Ick^{tm1a/+}$ and SAG-treated $Ick^{tm1a/tm1a}$ palates after 24 h in organ culture. (B, C, F, G) Expression patterns of *Ptch1* and *Gli1* in the developing palates after 24 h in organ culture. (D, H) Ki67-positive cells in the developing palates after 24 h in organ culture. Black dotted circles, remaining midline epithelial seam; black dotted line, the margin of the palatal epithelium. Scale bars, A–H: 50 μm.

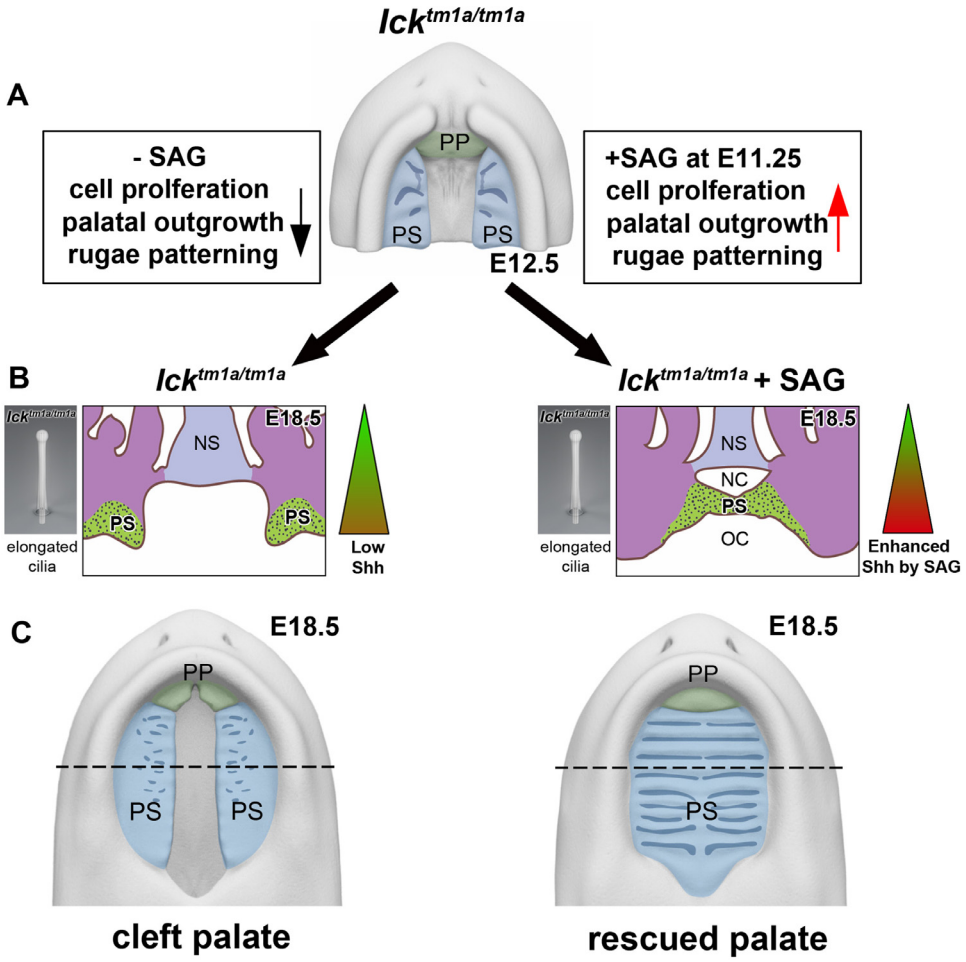

Fig. 8. Schematic diagram showing the effects of SAG treatment on cleft palate in the *Ick*$^{tm1a/tm1a}$ mice. (A) Effects of SAG treatment in the developing palates of *Ick*$^{tm1a/tm1a}$ embryos. (B, C) Schematic views showing the restoration of cleft palate in SAG-treated *Ick*$^{tm1a/tm1a}$ embryos. PP, primary palate; PS, palatal shelf; OC, oral cavity; NC, nasal cavity; and NS, nasal septum

cell proliferation by modulating the activity of the mammalian target of rapamycin (mTOR) complex 1 via phosphorylation of Raptor [33]. Thus, cell proliferation in the developing palate may be regulated by ICK function in cell cycle regulation in addition to cilia-mediated SHH signaling. However, our cell proliferation assay showed that activation of SHH signaling by SAG treatment is sufficient to promote cell proliferation in *Ick*$^{tm1a/tm1a}$ embryos (Fig. 7). Nevertheless, we cannot entirely exclude the possibility that other signaling pathways may also be affected by ICK deficiency and may contribute to the cleft palate phenotype as well. It will be interesting to examine if manipulating other signaling pathways in combination with SAG would increase the rescuing efficiency.

It was shown that *Ick* is expressed in the small and large intestines [34], and SHH directly regulates patterning and differentiation of the gastrointestinal tract [35, 36]. Consistent with these reports, *Ick*-deficient mutants also exhibited reduced stomach size, shortened intestines, and imperforate rectum (Fig. S4). We observed that SAG treatment at E11.25 restores the lengths of the small and large intestines and the imperforate rectum, but the reduced size of the stomach is not restored (Fig. S4). This discrepancy may be because developmental timing that requires SHH signaling is different in different tissues. Thus, it is crucial to determine the correct timing of pharmacological intervention to regulate the developmental signaling pathways according to the understanding of the precise developmental processes.

Taken together, this study suggests that pharmacologic intervention with a small chemical reagent offers a way to modulate developmental signaling pathways, enabling us to easily dissect the causative signaling pathway and reveal the mechanisms underlying the pathogenesis of genetic disorders. Moreover, further studies on other ciliopathies using signaling pathway-modulating agents will help us to better understand the fundamental mechanisms of the cilia-involved organogenesis and to increase the possibility of therapy for ciliopathies.

Funding Sources

This research was supported by the National Research Foundation of Korea Grant (NRF-2014M3A9D5A01073969 and NRF-2018R1A2B2008166 to H.W.K.; NRF-2016R1A5A2008630 and NRF-2017R1A2B3009133 to J.B; NRF-2016R1A6A3A11932191 to J.S; NRF-2018R1A5A2023127 to K.L) and by the Yonsei University Future Leading Research Initiative (2015-22-0058 to J.B). The funders of the study had no role in the study design, data collection, data analysis, data interpretation, or writing of the report.

Author Contributions

J. Bok and H.W. Ko led the study design and prepared the manuscript. J.O. Shin and J. Song carried out the experiments. H.S. Choi counted the EdU-positive cells and performed the statisti-

cal analysis. K. Lee and J. Lee synthesized the Smoothened agonist (SAG). All authors read and approved the final manuscript.

Declaration of Competing Interest

The authors have nothing to disclose.

CRediT authorship contribution statement

Jeong-Oh Shin: Funding acquisition, Investigation, Methodology, Visualization, Writing - original draft, Writing - review & editing. **Jieun Song:** Investigation, Methodology, Visualization, Writing - original draft, Writing - review & editing. **Han Seul Choi:** Investigation, Writing - review & editing. **Jisu Lee:** Resources, Writing - review & editing. **Kyeong Lee:** Funding acquisition, Resources, Writing - review & editing. **Hyuk Wan Ko:** Conceptualization, Supervision, Funding acquisition, Methodology, Visualization, Writing - original draft, Writing - review & editing. **Jinwoong Bok:** Conceptualization, Supervision, Funding acquisition, Methodology, Visualization, Writing - original draft, Writing - review & editing.

Acknowledgments

We thank Ms. Hyeon-Joo Kim for the schematic diagram.

Supplementary materials

Supplementary material associated with this article can be found, in the online version, at doi:10.1016/j.ebiom.2019.10.016.

References

[1] Lahiry P, Wang J, Robinson JF, Turowec JP, Litchfield DW, Lanktree MB, et al. A multiplex human syndrome implicates a key role for intestinal cell kinase in development of central nervous, skeletal, and endocrine systems. Am J Hum Genet 2009;84(2):134–47.
[2] Oud MM, Bonnard C, Mans DA, Altunoglu U, Tohari S, Ng AY, et al. A novel ICK mutation causes ciliary disruption and lethal endocrine-cerebro-osteodysplasia syndrome. Cilia 2016;5:8.
[3] Paige Taylor S, Kunova Bosakova M, Varecha M, Balek L, Barta T, Trantirek L, et al. An inactivating mutation in intestinal cell kinase, ICK, impairs hedgehog signalling and causes short rib-polydactyly syndrome. Hum Mol Genet 2016;25(18):3998–4011.
[4] Moon H, Song J, Shin JO, Lee H, Kim HK, Eggenschwiller JT, et al. Intestinal cell kinase, a protein associated with endocrine-cerebro-osteodysplasia syndrome, is a key regulator of cilia length and Hedgehog signaling. Proc Natl Acad Sci U S A 2014;111(23):8541–6.
[5] Tong Y, Park SH, Wu D, Xu W, Guillot SJ, Jin L, et al. An essential role of intestinal cell kinase in lung development is linked to the perinatal lethality of human ECO syndrome. FEBS Lett 2017;591(9):1247–57.
[6] Lan Y, Jiang R. Sonic hedgehog signaling regulates reciprocal epithelial-mesenchymal interactions controlling palatal outgrowth. Development 2009;136(8):1387–96.
[7] Habashi JP, Judge DP, Holm TM, Cohn RD, Loeys BL, Cooper TK, et al. Losartan, an AT1 antagonist, prevents aortic aneurysm in a mouse model of Marfan syndrome. Science 2006;312(5770):117–21.
[8] Shillingford JM, Murcia NS, Larson CH, Low SH, Hedgepeth R, Brown N, et al. The mTOR pathway is regulated by polycystin-1, and its inhibition reverses renal cystogenesis in polycystic kidney disease. Proc Natl Acad Sci U S A 2006;103(14):5466–71.
[9] Tobin JL, Beales PL. Restoration of renal function in zebrafish models of ciliopathies. Pediatr Nephrol 2008;23(11):2095–9.
[10] Lu S, Kanekura K, Hara T, Mahadevan J, Spears LD, Oslowski CM, et al. A calcium-dependent protease as a potential therapeutic target for Wolfram syndrome. Proc Natl Acad Sci U S A 2014;111(49):E5292–301.
[11] Ankamreddy H, Min H, Kim JY, Yang X, Cho ES, Kim UK, et al. Region-specific endodermal signals direct neural crest cells to form the three middle ear ossicles. Development 2019;146(2):167965 dev.
[12] Bok J, Dolson DK, Hill P, Ruther U, Epstein DJ, Wu DK. Opposing gradients of Gli repressor and activators mediate Shh signaling along the dorsoventral axis of the inner ear. Development 2007;134(9):1713–22.
[13] Shin JO, Lee JM, Cho KW, Kwak S, Kwon HJ, Lee MJ, et al. MiR-200b is involved in Tgf-beta signaling to regulate mammalian palate development. Histochem Cell Biol 2012;137(1):67–78.
[14] Goetz SC, Anderson KV. The primary cilium: a signalling centre during vertebrate development. Nat Rev Genet 2010;11(5):331–44.
[15] Cobourne MT, Green JB. Hedgehog signalling in development of the secondary palate. Front Oral Biol 2012;16:52–9.
[16] Bush JO, Palatogenesis Jiang R. morphogenetic and molecular mechanisms of secondary palate development. Development 2012;139(2):231–43.
[17] He F, Xiong W, Wang Y, Li L, Liu C, Yamagami T, et al. Epithelial Wnt/beta-catenin signaling regulates palatal shelf fusion through regulation of Tgfbeta3 expression. Dev Biol 2011;350(2):511–19.
[18] Snouffer A, Brown D, Lee H, Walsh J, Lupu F, Norman R, et al. Cell Cycle-Related Kinase (CCRK) regulates ciliogenesis and Hedgehog signaling in mice. PLoS Genet 2017;13(8):e1006912.
[19] Frank-Kamenetsky M, Zhang XM, Bottega S, Guicherit O, Wichterle H, Dudek H, et al. Small-molecule modulators of Hedgehog signaling: identification and characterization of Smoothened agonists and antagonists. J Biol 2002;1(2):10.
[20] Roper RJ, Baxter LL, Saran NG, Klinedinst DK, Beachy PA, Reeves RH. Defective cerebellar response to mitogenic Hedgehog signaling in down [corrected] syndrome mice. Proc Natl Acad Sci U S A 2006;103(5):1452–6.
[21] Heine VM, Griveau A, Chapin C, Ballard PL, Chen JK, Rowitch DH. A small–molecule smoothened agonist prevents glucocorticoid-induced neonatal cerebellar injury. Sci Transl Med 2011;3(105):105ra4.
[22] Chen JK, Taipale J, Young KE, Maiti T, Beachy PA. Small molecule modulation of Smoothened activity. Proc Natl Acad Sci U S A 2002;99(22):14071–6.
[23] Gritli-Linde A. Molecular control of secondary palate development. Dev Biol 2007;301(2):309–26.
[24] Fish EW, Parnell SE, Sulik KK, Baker LK, Murdaugh LB, Lamson D, et al. Preaxial polydactyly following early gestational exposure to the smoothened agonist, SAG, in C57BL/6J mice. Birth Defects Res 2017;109(1):49–54.
[25] Rice R, Spencer-Dene B, Connor EC, Gritli-Linde A, McMahon AP, Dickson C, et al. Disruption of Fgf10/Fgfr2b-coordinated epithelial-mesenchymal interactions causes cleft palate. J Clin Invest 2004;113(12):1692–700.
[26] Broekhuis JR, Verhey KJ, Jansen G. Regulation of cilium length and intraflagellar transport by the RCK-kinases ICK and MOK in renal epithelial cells. PLoS One 2014;9(9):e108470.
[27] Chaya T, Omori Y, Kuwahara R, Furukawa T. ICK is essential for cell type-specific ciliogenesis and the regulation of ciliary transport. EMBO J 2014;33(11):1227–42.
[28] Yi P, Xie C, Ou G. The kinases male germ cell-associated kinase and cell cycle-related kinase regulate kinesin-2 motility in Caenorhabditis elegans neuronal cilia. Traffic 2018;19(7):522–35.
[29] Maurya AK, Rogers T, Sengupta P. A CCRK and a MAK Kinase Modulate Cilia Branching and Length via Regulation of Axonemal Microtubule Dynamics in Caenorhabditis elegans. Curr Biol 2019;29(8) 1286-300 e4.
[30] Tian H, Feng J, Li J, Ho TV, Yuan Y, Liu Y, et al. Intraflagellar transport 88 (IFT88) is crucial for craniofacial development in mice and is a candidate gene for human cleft lip and palate. Hum Mol Genet 2017;26(5):860–72.
[31] Jeong J, Mao J, Tenzen T, Kottmann AH, McMahon AP. Hedgehog signaling in the neural crest cells regulates the patterning and growth of facial primordia. Genes Dev 2004;18(8):937–51.
[32] Das I, Park JM, Shin JH, Jeon SK, Lorenzi H, Linden DJ, et al. Hedgehog agonist therapy corrects structural and cognitive deficits in a down syndrome mouse model. Sci Transl Med 2013;5(201):201ra120.
[33] Wu D, Chapman JR, Wang L, Harris TE, Shabanowitz J, Hunt DF, et al. Intestinal cell kinase (ICK) promotes activation of mTOR complex 1 (mTORC1) through phosphorylation of Raptor Thr-908. J Biol Chem 2012;287(15):12510–19.
[34] Togawa K, Yan YX, Inomoto T, Slaugenhaupt S, Rustgi AK. Intestinal cell kinase (ICK) localizes to the crypt region and requires a dual phosphorylation site found in map kinases. J Cell Physiol 2000;183(1):129–39.
[35] Kolterud A, Grosse AS, Zacharias WJ, Walton KD, Kretovich KE, Madison BB, et al. Paracrine Hedgehog signaling in stomach and intestine: new roles for hedgehog in gastrointestinal patterning. Gastroenterology 2009;137(2):618–28.
[36] Mao J, Kim BM, Rajurkar M, Shivdasani RA, McMahon AP. Hedgehog signaling controls mesenchymal growth in the developing mammalian digestive tract. Development 2010;137(10):1721–9.